

An integrated open population distance sampling approach for modelling age-structured populations

Erlend B. Nilsen^{1,2,*} & Chloé R. Nater¹

1: Department for Terrestrial Biodiversity, Norwegian Institute for Nature Research (NINA), 7034 Trondheim, Norway

2: Faculty of Biosciences and Aquaculture (FBA), Nord University, 7713 Steinkjer, Norway

* correspondence: erlend.nilsen@nina.no

ORCID: EBN: 0000-0002-5119-8331; CRN: 0000-0002-7975-0108

Abstract

*Estimation of abundance and demographic rates for populations of wild species is a challenging but fundamental issue for both management and research into ecology and evolution. One set of approaches that has been used extensively to estimate abundance of wildlife populations is Distance Sampling (DS) methods for line or point transect survey data. Historically, DS models were only available as closed population models, and did not allow for the estimation of changes in abundance through time. The advent of open population formulations based on the DS framework greatly extended the scope of the models, but much untapped potential remains in models that estimate temporal dynamics not only in abundance but also in the underlying demographic rates. Here, we present an integrated distance sampling approach that utilize age-structured survey data and auxiliary data from marked individuals to jointly estimate population density and the demographic rates (recruitment rate and survival probability) that drive temporal changes density. The core of the resulting model is, in essence, equivalent to both an integrated population model and a matrix population model with two age classes: juveniles and adults. The integrated framework allows making full use of the available data by effectively combining line transect and telemetry data, and can easily be adapted to include additional and/or different data types. Moreover, as demographic rates often respond to environmental variation, our approach also supports direct estimation of the effects of such environmental covariates on demographic rates. Through a comprehensive simulation study we show that the model is able to adequately recover true population and vital rate dynamics. Subsequent application to data from a study of willow ptarmigan (*Lagopus lagopus*) in Norway showcases the frameworks ability to recover both fluctuations and trends in population dynamics and highlights its potential applicability to a wide range of species surveyed using distance sampling approaches.*

35 1. Introduction

36 Estimating abundance and demographic rates for wildlife populations is an integral part of
37 basic and applied ecology (Skalski, Ryding, and Millspaugh 2005; Williams, Nichols, and
38 Conroy 2002). Over the last few decades, tremendous progress has been made towards this
39 end. This progress is partly driven the development and application of new field data
40 collection methods and approaches, such as citizen science data (Danielsen et al. 2022),
41 camera trap data (Hamel et al. 2013) and the collection of environmental DNA data (Beng
42 and Corlett 2022). In addition, developments of novel statistical methods alongside
43 decreases in computational costs now allow researchers to estimate abundance and
44 demographic rates in situations where it was not feasible before (Zipkin et al. 2021).
45 Combined, these advances put us in a much better position for estimating quantities needed
46 for population management (Williams, Nichols, and Conroy 2002) and indices relevant for
47 large scale policy applications, e.g. Essential Biodiversity Variables (Kissling et al. 2018).

48 Until recently, joint estimation of population dynamics and demography has relied mostly
49 on data from marked individuals and associated open-population capture-mark-recapture
50 models (Schaub and Kery 2021). While such methods can provide valuable information for
51 both ecological research and management, collecting the necessary data is typically costly
52 and logistically challenging to implement over large areas. Monitoring programmes
53 focusing on abundance trends over larger areas, on the other hand, are typically based on
54 data from unmarked animals. One often used approach for such surveys is to structure data
55 collection around the distance sampling (DS) method. DS has been used for estimating
56 animal abundance in a wide range of contexts and for a variety of taxa (Buckland et al.
57 2015). One reason for the method's popularity is that it does not require repeated visits to
58 the same sites for estimating detection probability. This makes DS particularly useful for
59 implementation in participatory monitoring programs, allowing stakeholders to take part in
60 the data collection process.

61 The most common implementations of DS models have long used closed-population
62 formulations, and thus do not allow formulating a process model that projects abundance
63 across years based on estimates of population growth rate (λ) or underlying demographic
64 rates Buckland et al. (2015). In recent years, DS approaches have been extended in many
65 ways, including applications that estimate changes in abundance over time in open
66 populations via a hidden state model representing population dynamics (Moore and Barlow
67 2011; Sollmann et al. 2015; Schaub and Kery 2021). This has greatly extended the potential
68 of DS approaches for studying ecological dynamics across time and space. However, while
69 these latter frameworks may allow to accurately quantify population changes, they typically
70 provide little information on the drivers of these changes, i.e. the underlying vital rates. In
71 fact, if the data does not contain information about the age (and/or sex-) structure of the
72 surveyed population, there is no straightforward way to estimate demographic rates from
73 such data. On the contrary, if age (and sex) of detected individuals can be determined, this
74 information can be used to provide information on recruitment rates and survival
75 probabilities. Nilsen and Strand (2018), for example, used a model based on harvest
76 statistics and observations of population age structure to estimate population abundance
77 and demographic rates without the need for any additional data from marked individuals.

78 Concurrent with the development of more sophisticated DS models, another group of
79 models has emerged and rapidly gained popularity, not least for their ability to disentangle
80 demographic processes underlying population dynamic: integrated population models
81 (IPMs, Schaub and Kery 2021). Through joint analysis of multiple datasets, IPMs allow
82 simultaneous estimation of population size and composition, as well as all vital rates that
83 form part of an underlying age- or stage-structured population model. Since both DS models
84 and IPMs estimate population size/density, a combination of the two frameworks has the
85 potential to provide good estimates of both population- and demographic parameters by
86 maximizing knowledge gained from transect surveys by augmenting them with other
87 available data (e.g. Schmidt and Robison 2020).

88 In this study, we present a new IPM (IDSM, integrated distance sampling model) which
89 integrates data from line transect distance sampling survey data and survival data from
90 marked birds. The model's core is a stage-structured matrix population model that projects
91 population size from one time step to the next based on underlying survival and
92 recruitment rates. Below, we first present the model and assess its robustness and
93 performance through application to simulated data. We then apply the model to real data
94 collected from a willow ptarmigan (*Lagopus lagopus*) study in Central Norway. Because
95 demographic rates are often affected by environmental covariates (e.g. rodent abundance in
96 the case of willow ptarmigans), we also illustrate how such covariates can be included in
97 the modelling framework.

98
99

100 2. Methods

101 2.1 An integrated distance sampling model

102 Our open population integrated distance sampling model (IDSM) consists of two major
103 components: a latent structured population model and a set of likelihoods for data
104 originating from distance sampling surveys and auxiliary survival monitoring. In the
105 example case, these auxiliary data come from a radio-telemetry study, but in principle other
106 types of capture-recapture data can also be used.

107 2.1.1 Age-structured population model

108 The population model follows a post-breeding census and includes two age classes:
109 juveniles (young of the year) and adults (> 1 year of age, [Figure 1](#)). This structure is
110 inspired by earlier models for our focal species, the willow ptarmigan (+ref), and is
111 commonly used for populations of passerine and game birds (Williams, Nichols, and Conroy
112 2002; Schaub and Kery 2021). In the context of our willow ptarmigan case study (see
113 below), the census falls into late summer and coincides with the annual distance-sampling
114 survey in August.

115 Both juveniles and adults survive from year t census to year $t + 1$ census with survival
116 probability S_t . As ptarmigan can reproduce already as 1-year old, all survivors then produce
117 offspring in late June which recruit into the population as juveniles just prior to the census
118 in year $t + 1$ according to a recruitment rate R_{t+1} . The changes in densities (numbers) of
119 juveniles and adults in the population, D_{juv} and D_{ad} , can thus be expressed as

$$\begin{aligned} 120 \quad D_{juv,t+1} &= D_{ad,t+1} * R_{t+1} \\ D_{ad,t+1} &= S_t * (D_{juv,t} + D_{ad,t}) \end{aligned}$$

121 or, alternatively, in matrix notation as

$$122 \quad \begin{bmatrix} D_{juv,t+1} \\ D_{ad,t+1} \end{bmatrix} = \begin{bmatrix} S_t * R_{t+1} & S_t * R_{t+1} \\ S_t & S_t \end{bmatrix} \begin{bmatrix} D_{juv,t} \\ D_{ad,t} \end{bmatrix}$$

123 Note that recruitment rate R is defined as juveniles/adult (not juveniles/female). We also
124 make the simplifying assumption that there is no age- or sex-dependence of vital rates, but
125 this assumption could be relaxed by including additional auxiliary data (Israelsen et al.
126 2020; Sandercock et al. 2011).

141

$$esw_t = \sqrt{\frac{\pi * \sigma_t^2}{2}}$$

$$\hat{p}_t = esw_t / W$$

142 The average detection probability \hat{p}_t is an integral part of the second data likelihood which
 143 relates the observed number of animals in each age class a , $obsN_{a,j,t}$ (j = transect) to the
 144 corresponding true number per transect, $N_{a,j,t}$:

$$145 \quad obsN_{a,j,t} \sim Poisson(\hat{p}_t * N_{a,j,t})$$

146 $N_{juv,j,t}$ and $N_{ad,j,t}$ are then linked back to the population model by converting them to
 147 densities through multiplication with $2L_{j,t}W$ (where $L_{j,t}$ is length of transect j in year t , and
 148 W is the truncation distance).

149 The third data likelihood focuses on the counts of adults ($obsAd_{j,t}$) and juveniles ($obsJuv_{j,t}$)
 150 observed during the distance sampling surveys and links them to year-specific recruitment
 151 rate:

$$152 \quad obsJuv_{j,t} \sim Poisson(R_t * obsAd_{j,t})$$

153 *2.1.3 Likelihood for radio-telemetry data*

154 The final likelihood is for the auxiliary telemetry data. It is set up under the assumption of
 155 perfect detection, and hence known fates, of animals bearing transmitters and links the
 156 numbers of animals released at the start of season k of year t to the number of survivors at
 157 the end of the same season:

$$158 \quad survivors_{k,t} \sim Binomial(released_{k,t}, Sk_t)$$

159 Here, Sk_t is the seasonal survival probability, and annual survival probability, S_t is
 160 calculated as $S1_t * S2_t$.

161 *2.1.3 Hierarchical models with time-variation in parameters*

162 Vital rates (survival probabilities S , recruitment rates R) and detection parameters (half-
 163 normal detection parameters σ) can all be modelled as time-dependent in our framework.
 164 For both the tests with simulated data and the case study described below, we implemented
 165 log-normally distributed random year effects on all parameters except survival, which was
 166 set to be constant. In the case study, we additionally included an effect of rodent occupancy
 167 (see details below) on log recruitment rates, resulting in the following model:

$$168 \quad \log(R_t) = \log(\mu_R) + \beta * RodentOcc_t + \epsilon_t$$

169 where μ_R is the baseline recruitment rate, β the slope of the effect of rodent occupancy, and
 170 ϵ_t the normally distributed random effects.

171 2.2 Model testing with simulated data

172 We assessed the model's overall performance and ability to estimate abundance,
173 demographic rates, and detection parameters without bias by testing it on simulated data.
174 We generated a total of 10 simulated datasets in five steps. First, we simulated 15-year
175 time-series of survival and recruitment rates from biologically plausible values for averages
176 and – in the case of recruitment – among-year variation in demographic rates (survival was
177 held constant across years). Second, we used the yearly demographic rate and realistic
178 initial population densities to simulate stochastic population dynamics in 50 distinct sites.
179 Third, we simulated the grouping of individuals in each site by first determining the
180 expected number of groups in a site (based on the average group size of 5.6 from our
181 ptarmigan data) and then distributing individuals among groups via multinomial trials.
182 Fourth, we assigned a distance from transect line to each group and simulated the line
183 transect survey in all 50 sites across 15 years. Finally, we simulated 5-year time-series of
184 radio-telemetry data (= survival from one year to the next) for a subset of individuals (30
185 per year on average) using the simulated survival probabilities for each relevant year. We
186 then fit the IDSM to each of the 10 simulated datasets three times, using distinct seeds for
187 both simulating initial values and initiating and running the MCMC. Model implementation
188 for simulated data tests was largely identical to that for real data and is described in detail
189 below.

190 2.3 Case study

191 The willow ptarmigan has a circumpolar distribution (Fuglei et al., 2020), and lives year-
192 round in heterogeneous alpine and arctic ecosystems. In Norway, there has been a long-term
193 decline in the willow ptarmigan abundance across more than a century (Hjeljord and Loe
194 2022), but in the last few decades abundance trends has fluctuated both in time and space.
195 In Scandinavia, willow ptarmigan is a valued game species (see e.g. Andersen et al. (2014)),
196 and there have been several long-term research projects devoted to understanding how
197 they respond to environmental variation and harvest management (Israelsen et al. 2020;
198 Sandercock et al. 2011). A key insight from across several study areas is the the annual
199 recruitment rate (i.e. R_t in our model, as outlined above) is highly variable, and is affected
200 both by spring conditions (Eriksen et al. 2023) and the abundance of small rodents, which
201 constitute alternative prey for common predators (i.e. the Alternative Prey Hypothesis; see
202 Hagen (1952); Kausrud et al. (2008); Bowler et al. (2020)). Adult survival show less inter-
203 annual fluctuations (Israelsen et al. 2020), although spatial (and potentially temporal)
204 variation due to e.g. harvest management is evident when comparing across studies
205 (Israelsen et al. 2020).

206 Our case study was based on an ongoing long-term research project on willow ptarmigan in
207 Lierne municipality in Central Norway (approximately 62.4 degrees north and 13.2 degrees
208 east). The study area is located in a sub-alpine ecosystem, and the landscape is a mosaic of
209 open heath and shrub vegetation (dominated by Ericacea, willow shrub *Salix spp.*, and
210 dwarf birch *Betula nana*), interspersed with bogs and forest patches (mainly birch *Betula*
211 *spp.*). The climate is strongly seasonal, with snow typically covering the ground from
212 October/November through April/May.

213 From this study system, two datasets were used for the case study:

- 214 1. Data from a line transect survey program targeting willow ptarmigan operated
215 under the natural resources management authorities (2007-2021, ongoing)
- 216 2. Data from an individual-based monitoring programme based on radio collared
217 willow ptarmigan (2015-2021, ongoing)

218 Line transect survey data were collected in August each year, prior to the annual autumn
219 harvest season, as part of the program “Hønsfuglportalen”. Hønsfuglportalen is a national
220 program for line transect surveys of tetraonid birds, and the effort is directed mainly
221 towards willow ptarmigan habitats. In our case study, we used data from the western part
222 of Lierne municipality. Line transects are surveyed by trained volunteers that use pointing
223 dogs to locate the birds. When located, the geographical coordinate, perpendicular distance
224 from the sampling line, the number of birds in the group, as well as the age (juvenile or
225 adult) and sex of the birds are recorded. As the surveys are conducted in early August,
226 juveniles can be distinguished from adults by their smaller body size. Males and females are
227 mainly distinguished by the sound (males often make a characteristic sound when being
228 flushed. Nevertheless, mis-identification can occur, and in addition a proportion of the birds
229 are registered as “unknown” age and/or sex. Since 2019, data has been collected through a
230 mobile app tailor-made for this project, which is available through App Store (for ios
231 phones) and Google Play (for Android phones). Before 2019, field workers reported their
232 data through a dedicated web portal. After data are collected and reported, they undergo
233 several steps of quality control: first by local contacts and subsequently by personnel at the
234 Norwegian Institute for Nature Research (NINA). The data are then standardized based on
235 the Darwin-Core standard (Wieczorek 2012), and made publicly available as a sampling-
236 event data set published through GBIF (Nilsen et al. 2023). For additional description of the
237 data collection procedures, see (Bowler et al. 2020; Kvasnes, Pedersen, and Nilsen 2018;
238 Nilsen et al. 2023).

239 The individual longitudinal study based on radio collared willow ptarmigan was conducted
240 in 2015-2021. Each winter (in February-March), willow ptarmigan were located at night
241 using snowmobiles and large hand nets with prolonged handles, as described in (Israelsen
242 et al. 2020). To prevent birds from flying off before the field personnel were close enough to
243 capture them, a high-powered head lamp was used to dazzle the birds. After capture, birds
244 were placed in an opaque bag to reduce stress. They were then fitted with a uniquely
245 numbered leg ring (~ 2.4g) and a Holohil RI-2BM or Holohil RI-2DM radio transmitter (~
246 14.1g) and subsequently released. The radio transmitters had an expected battery lifetime
247 of 24 months (RI-2BM) or 30 months (RI-2DM), and included a mortality circuit that was
248 activated if a bird had been immobile for 12 hours. We monitored the birds throughout
249 most of the year by triangulation from the ground at least once a month for 10 months of
250 the year (February – November) by qualified field personnel. If a mortality signal was
251 emitted from a transmitter, we attempted to recover it as soon as possible to determine
252 cause of death. A number of birds dispersed out of the main study areas and was thus out of
253 signal range for field personnel on the ground. To avoid loss of data, we conducted aerial
254 triangulation using a helicopter or airplane three times a year (May, September and
255 November) in the years 2016-2020.

256 **2.4 Bayesian model implementation**

257 We implemented the model in a Bayesian framework using NIMBLE version 1.0.1 (Valpine
258 et al. 2017) in R version 4.3.1 (R Core Team 2023). The likelihood for line transect
259 observation distances was set up using a custom half-normal distribution developed by
260 Michael Scroggie as part of the “nimbleDistance” package
261 (<https://github.com/scrogster/nimbleDistance>). We used non-informative uniform priors
262 (with biologically reasonable boundaries where possible) for all parameters. We assumed
263 constant survival and time-varying recruitment rate in models fit to both simulated and real
264 data.

265 For the model fits to simulated and real data we ran 3 and 4 MCMC chains with NIMBLE’s
266 standard samples for 500k and 100k iterations, respectively. 300k and 40k and thereof
267 were discarded as burn-in prior to thinning with factors 5 and 20 , leaving us with 40k and
268 3k posterior samples per chain (total of 120k and 12k samples per run), respectively.
269 Posterior samples from the model fitted to real data are available at Nilsen and Nater
270 (2024) (in folder PosteriorSamples_LierneCaseStudy).

271

272 **3. Results**

273 **3.1 Model performance on simulated datasets**

274 Posterior distributions for parameters estimated in three model fits to each of 10 simulated
275 data sets are shown in Figure 2 and Figure 3. Overall, the IDSM was able to correctly
276 estimate both detection parameters and demographic rate parameters from all 10
277 simulated datasets without any systematic bias. The replicate runs for each dataset resulted
278 in very similar posterior distributions, demonstrating that the models converged towards
279 the same posterior distributions irrespective of starting values. Estimates of population
280 sizes / densities were also adequate, and are presented in the supplementary materials
281 (available at Nilsen and Nater (2024) in folder SimCheck_byDataSet).

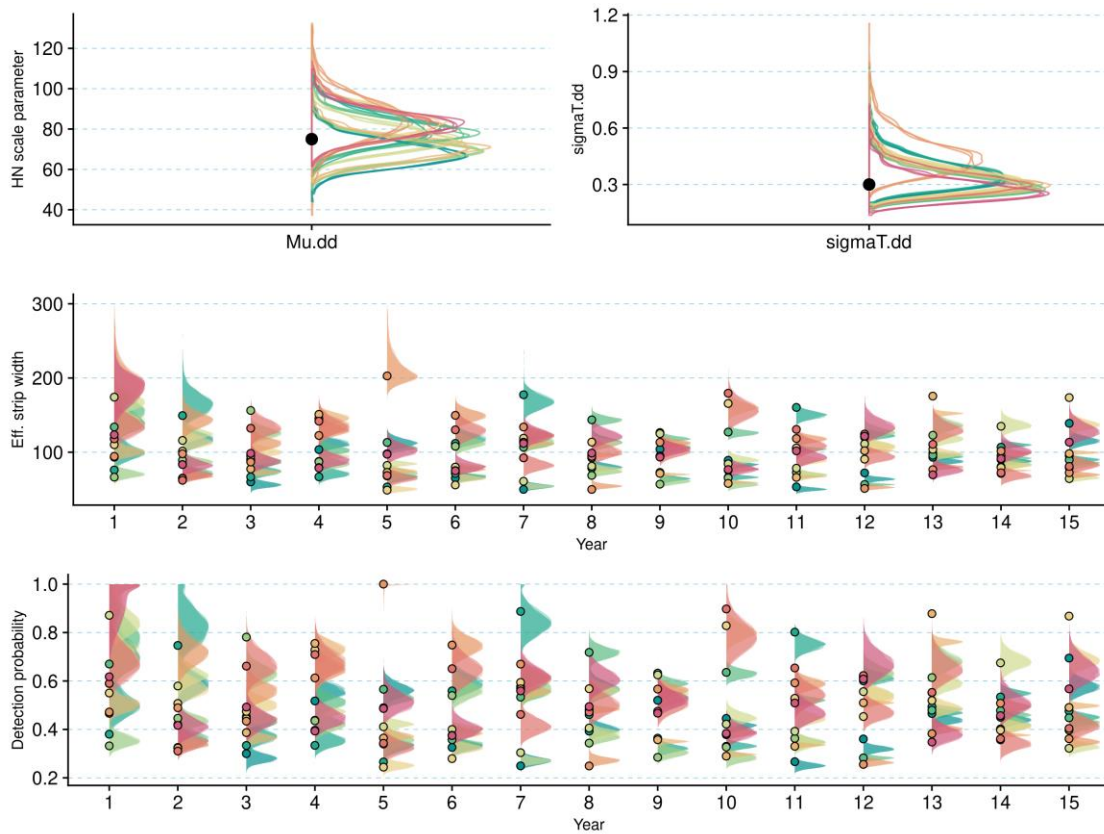


Figure 2: Detection parameters estimated from 10 distinct sets of simulated data (= colors). Upper panel depicts model parameters, and lower panels show derived estimated of effective strip width and mean detection probability. Dots represents true values (black for global values, colored for dataset-specific values), and density plot represent the posterior distributions for each model run.

282

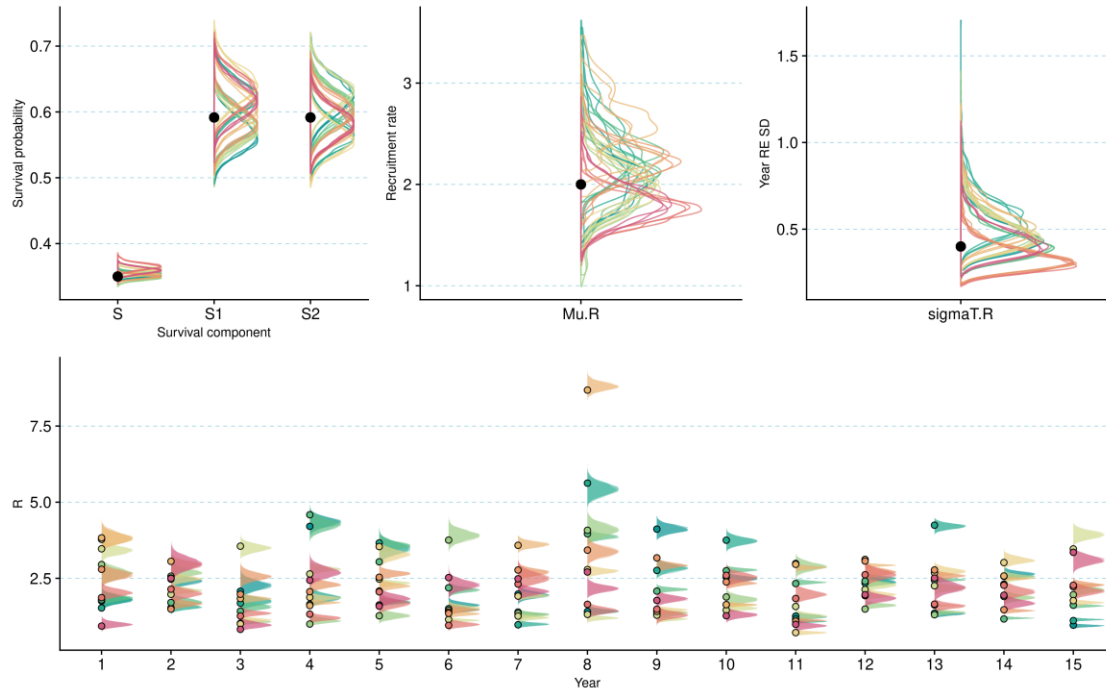


Figure 3: Demographic rate parameters estimated from 10 distinct sets of simulated data (= colors). Upper panel show annual and seasonal survival probabilities, hyperparameters for the random effects model for recruitment (mean and sd), and lower panel show annual estimates of the recruitment rate. Dots represent true values (black for global values, colored for dataset-specific values), and density curves represent the posterior distributions from each model run.

283 3.2 Case study on willow ptarmigans in Central Norway

284 Having evaluated the overall performance of our model on simulated data, we used data
 285 from our case study in Lierne as a case study to estimate abundance, vital rates and
 286 detection probabilities from a real-world data set. Ptarmigan population density increased
 287 markedly across the study period, from < 10 ptarmigan / km^2 in 2007 to > 35 ptarmigan /
 288 km^2 in 2021 (Figure 4). The increase was most distinct from 2016 and onward.

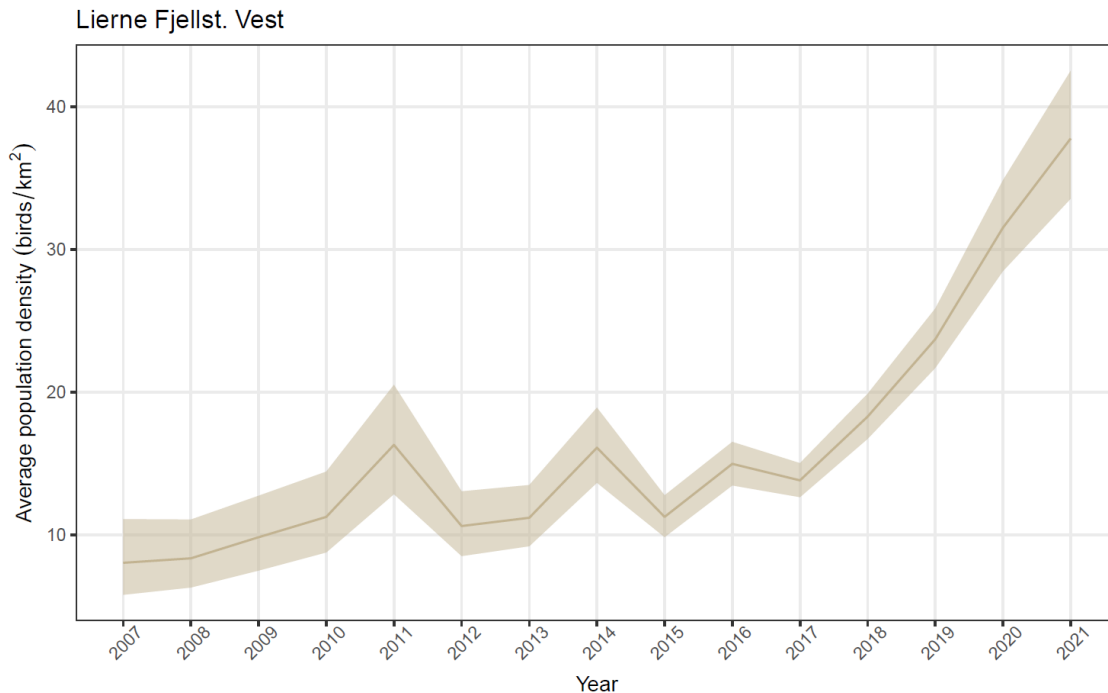


Figure 4: Estimated density of willow ptarmigans in Lierne from 2007 to 2021. Solid line represents the posterior median, ribbon marks 95% credible interval.

289 Average survival probability for August - January (S_1) was estimated at 0.46 (95% C.I = 0.42
 290 - 0.51) while average survival probability for February - July (S_2) was estimated as 0.64
 291 (95% C.I = 0.59 - 0.7) (Figure 5 A). Annual survival probability S , given by the product of S_1
 292 and S_2 , was estimated at 0.3 (95% C.I = 0.29 - 0.31), Figure 5 A).

293 Recruitment (R_t) was allowed to vary across years (see model specification), and estimates
 294 displayed large inter-annual variability (Figure 5 C, Figure S1). While the mean (baseline)
 295 recruitment μ_R was estimated as 2.9 (95% C.I = 2.5 - 3.4) the yearly recruitment rates
 296 ranged from 1.2 in year 2012 to 4.9 in year 2007.

297 Given the available data, the IDSM was not able to estimate a clear effect of small rodent
 298 abundance on ptarmigan recruitment (slope-parameter for the z-standardized rodent
 299 occurrence data = 0.037 ; 95% C.I. = -0.216 - 0.248, see supplementary figure
 300 "Rep_betaR.R.png" in Nilsen and Nater (2024)).

Lierne Fjellst. Vest

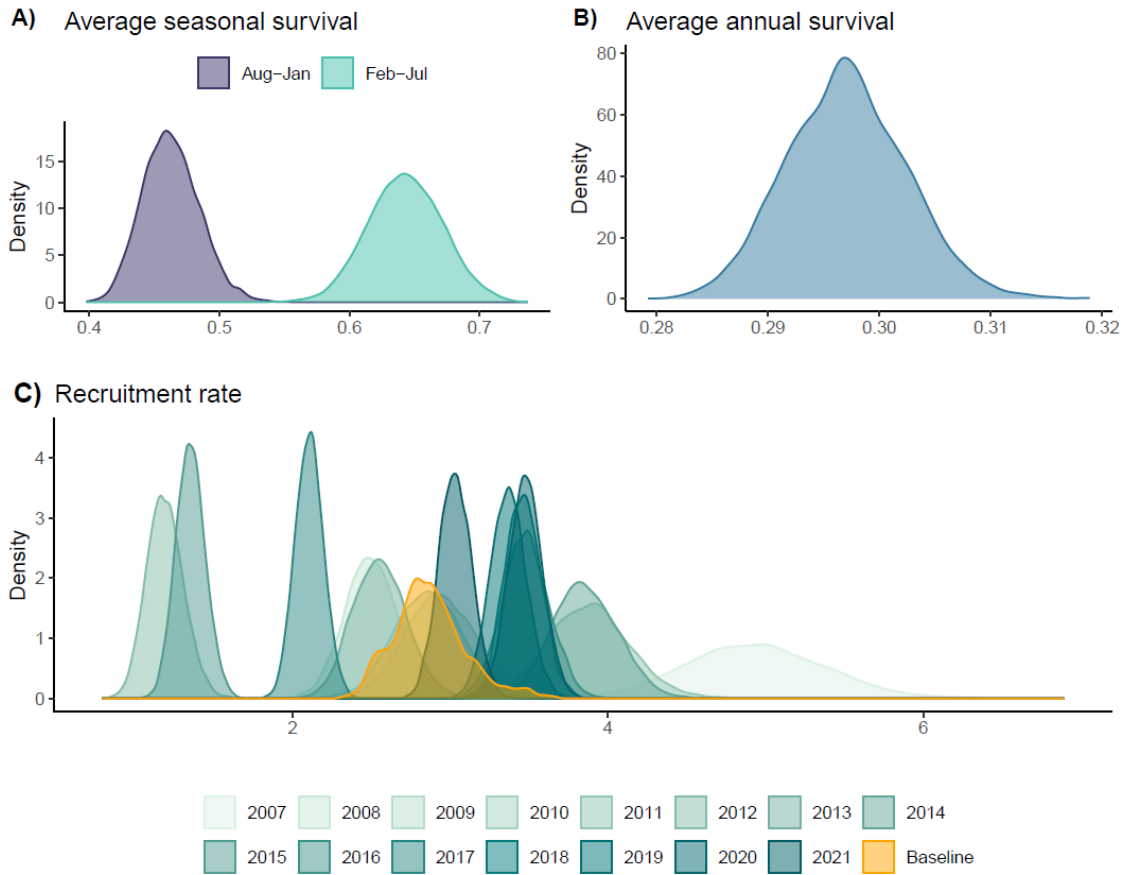


Figure 5: Posterior densities of A) seasonal survival, B) average annual survival, and C) recruitment rate. For the latter, the yellow distribution is for the intercept, representing a baseline recruitment rate when rodent occupancy is low. The turquoise distributions are for year-specific estimates or recruitment rate, with darker colors indicating later years.

301

302

303 Discussion

304 We developed an integrated population model that jointly analyses line transect distance
305 sampling survey data and data from marked individuals to estimate population abundance,
306 survival probabilities, and recruitment rates over time. We first used simulated data to
307 examine the model's ability to recover the underlying parameters when they were known.
308 We then fitted the model to data from an ongoing field study on willow ptarmigan in
309 Norway to showcase its applicability to real wildlife monitoring data.

310 Open population formulations of the distance sampling model have previously been
311 presented (Sollmann et al. 2015; Bowler et al. 2020; Moore and Barlow 2011), and in these
312 studies also applied to various ecological systems. The model presented here extends those
313 previous applications by formulating the underlying population process model as a stage-
314 structured matrix model (Caswell 2000) in which the matrix elements are represented by
315 annual survival probabilities and recruitment rates. While this has been the common
316 approach for a range of other statistical modelling frameworks, including the growing suite
317 of models falling into the category of integrated population models (Schaub and Kery 2021),
318 the integration of mechanistic population models into distance sampling frameworks is
319 rather new. The resulting modelling framework allow us to make maximum use of distance
320 sampling data in combination with auxiliary information both from the distance sampling
321 survey itself (i.e. information on age, sex, etc. of observed animals) and from other types of
322 monitoring, and enables estimation not only of changes in population density but also of
323 underlying vital rates over time.

324 In general, the model did a very good job at recreating the underlying parameters when
325 fitted to simulated data where the true values are known. The simulated data sets were
326 based on relatively wide ranges of parameter values, yet we did not find the model to have
327 any particular problems or biases recovering the original parameters used in simulations.
328 When the input data are unbiased (with respect to the underlying model formulation) we
329 therefore consider the model to be able to extract unbiased and meaningful demographic
330 parameters from age-structured distance sampling data.

331 Real data, however, are likely to be subject to certain biases, and such biases might result in
332 biased parameter estimates unless accounted for. One type of bias that is likely to be
333 common for age-structured distance sampling data arises from failure to (correctly) classify
334 the age class of observed individuals. In our case study on willow ptarmigan in Norway,
335 such misclassification is likely to happen at an unknown rate, even if the size difference
336 between adult and juvenile birds are quite substantial during the survey. Moreover, The
337 probability for misclassification might be related to both the timing of the survey (e.g. mid
338 August rather than early August), it might vary between observers, and even by survey
339 conditions. Observations with incorrectly classified age have the potential to introduce bias
340 in the IDSMs relative estimates of survival and recruitment. This is due to the way it uses
341 the distance sampling data to estimate survival and recruitment rates. In our process
342 model, the population growth rate (λ) is determined by the survival and recruitment rate in
343 the following way: $\lambda = S + (S * R)$, and this creates a dependence between the
344 demographic parameters. If the age ratio in the data are biased or contain frequent
345 misclassifications, this is likely to affect the relative contribution of survival and

346 recruitment to the growth rate. To get an idea of the potential effect of this on parameter
347 estimation, we checked the sensitivity of the output of the model fit to real data with regard
348 to the treatment of birds classified as “unknown sex and age” by the field personnel (see
349 Methods). In the model version presented in the results section, we made the assumption
350 that these birds were in fact juveniles. Comparing estimates to an alternative scenario in
351 which we discarded all birds classified as “unknown sex and age” (see supplementary
352 figures in Nilsen and Nater (2024)) we found that – as expected – estimated population
353 density was virtually unaffected by the treatment of “unknown sex and age” observations,
354 while the annual demographic parameters shifted proportional to the amount of “unknown
355 sex and age” observations in the given year (towards higher recruitment and lower
356 survival). Thus, biases in the reported age ratios may affect estimated of demographic rates,
357 but not so much population density. Since the proportion of “unknown sex and age”
358 observations in our ptarmigan case study was rather low, potential biases in estimates
359 resulting from age misclassification are expected to be small. Nonetheless, future
360 developments of the IDSM modelling framework should focus on ways of accounting
361 explicitly for misclassification of age class in the field.

362 The density estimates that we derived from the case study on Willow ptarmigan in Norway
363 is comparable to previous estimates from across Norway (see e.g. Sandercock et al. (2011);
364 Kvasnes, Pedersen, Solvang, et al. (2014)). Throughout the study period from 2007 - 2021,
365 the density increased markedly, but the reason for this increase is not known. Compared to
366 previous studies on ptarmigan (see e.g. (Israelsen et al. 2020; Sandercock et al. 2011)), we
367 could have expected somewhat higher estimates of survival probability. One potential
368 reason for the overall lower estimates obtained here is that our IDSM analysis assumed
369 constant survival over the period 2007-2021 while survival, in reality, may have changed
370 over time. If survival in more recent years, when telemetry data was collected (and the
371 study of e.g. Israelsen et al. (2020) was carried out) was higher than in earlier years –
372 something that seems likely given population increase over recent years – an average over
373 the entire time period is expected to be lower. On a different note, we can also not exclude
374 the possibility of a small degree of bias in survival estimates due to misclassification of age
375 in the data (see above), especially seeing as the IDSM’s recruitment rate estimates also
376 appear somewhat high compared to other studies on willow ptarmigan (Eriksen et al. 2023;
377 Kvasnes, Pedersen, Storaas, et al. 2014; Steen et al. 1988). Note however that the last period
378 of the study period in Lierne, there was substantial increase in the density (ref Figure 2),
379 which might indicate that the recruitment and/or survival rates were high in this period.

380 In addition to estimating demographic rates from line transect data, the IDSM also allows
381 including relevant environmental effects on the demographic rates themselves, and not just
382 on population growth rate as a whole (λ). In the ptarmigan case study we thus attempted to
383 investigate the effect of small rodent abundance (approximated as the proportion of
384 transect lines on which rodents were reported each year) on recruitment rate.
385 Unfortunately, we were not able to detect a clear effect of rodent abundance due to large
386 uncertainty associated with the estimate (see supplementary figures in Nilsen and Nater
387 (2024)). This may seem somewhat surprising given that such a pattern has been reported
388 repeatedly in the literature (see e.g. Bowler et al. (2020)). We speculate that there are at
389 least three potential (non-mutual) explanations to this result. The first is that our covariate

390 data may not have been well suited for estimating effects on recruitment. The data on
391 rodent abundance was heavily zero-inflated, and the annual variation in the index was
392 rather small otherwise, making for a covariate with relatively little information content.
393 While this may be partially a consequence of how these data are collected, it is also well
394 known that the amplitude and regularity of the rodent cycles has been fading in recent
395 decades (Kausrud et al. 2008; Cornulier et al. 2013), and our study area might be no
396 exception. Lack of peak rodent years in the time series to which we fitted the model may
397 thus also have contributed to making effect estimation challenging. Second, it is possible
398 that rodent effects were obscured by other, potentially stronger, covariate effects. Previous
399 research has shown that ptarmigan recruitment is also sensitive to the weather in the late
400 winter and spring (before and during the breeding season); as we did not fit any weather
401 covariates to the model so there is a possibility that strong unaccounted for effects of spring
402 conditions in certain years may have masked any remaining effects of small rodent
403 abundance. Finally, the data set used in this analysis is relatively short (15 years), leaving us
404 with somewhat limited statistical power to detect effects of temporal covariates . Taken
405 together we therefore do not consider this study as a particularly strong test of the
406 underlying effect of small rodent fluctuations on ptarmigan recruitment rates. It is worth
407 noting that future applications could increase statistical power by including either more
408 years of data or capitalizing on space-for-time substitution as the Norwegian ptarmigan
409 monitoring programme spans many more locations beyond Lierne. Bowler et al. (2020), for
410 example, used data from the same sampling program but from more areas using a simpler
411 open population DS model, and detected a very clear signal from small rodent abundance
412 on ptarmigan population growth rate. An extension of our IDSM to include data from
413 multiple areas therefore constitutes a promising approach for investigating to which extent
414 similar results emerge by linking environmental covariates to the actual demographic rates
415 and not only just to the resulting population growth rates.

416 The new IDSM framework presented here is relevant for many wildlife populations that are
417 surveyed using line transect sampling that includes additional information on age, sex,
418 and/or life stages of the observed individuals. Following the integrated modelling
419 philosophy, the IDSM also allows for the integration of auxiliary data. In our application
420 here, we integrated data from radio-telemetry of marked birds, which explicitly supported
421 the estimation of survival probabilities. The IDSM framework is very flexible, however, and
422 open to the inclusion of additional/other auxiliary data that contains information on
423 demographic rates or population size/density. Moreover, hierarchical nature of the model
424 makes is straight forward to adapt to different species and to include different suites of
425 environmental covariates on the demographic rates. Finally, it constitutes a modelling
426 framework that is well suited for extension to multiple areas and thus able to capitalize on
427 space-for-time substitution to produce large-scale and spatially explicit estimates of
428 population density, demographic rates, and environmental effects from large-scale
429 (participatory) monitoring.

430 **Author contributions**

431 EBN Lead - Drafted the model code; Lead - Wrote first version of ms; Lead - Data collection;
432 Contributed - Modelling and analyses

433 CRN Lead - Updated, further developed, and finalized model code; Lead - Modelling and
434 analyses; Contributed - Wrote first version of ms

435 **Acknowledgements**

436 We are grateful to field workers that collected the line transect data through the
437 Hønsfuglportalen program. Fjellstyrene i Lierne and many colleagues from NINA and Nord
438 University contributed both to the line transect program and the field work related to the
439 marked willow ptarmigan. We also thank James A. Martin for constructive discussions
440 during the later stages of this work.

441 **Funding**

442 Both data collection and analytical work were financed by the Norwegian Environment
443 Agency funded the projects (grant nrs 17010522, 19047014 and 22047004).

444 **Conflict of interest disclosure**

445 The authors declare that they comply with the PCI rule of having no financial conflicts of
446 interest in relation to the content of the article

447 **Data and code availability**

448 The raw data from the line transect surveys is deposited on GBIF and can be accessed freely
449 via the Living Norway Data Portal (<https://data.livingnorway.no>). The work here is based
450 on version 1.7 of the dataset “Tetraonid line transect surveys from Norway: Data from
451 Fjellstyrene” (Nilsen et al. 2023).

452 The auxiliary radio-telemetry data and rodent occupancy data, and all code used for
453 wrangling, analysing, and visualizing data and results can be found in the project’s
454 repository on GitHub: https://github.com/ErlendNilsen/OpenPop_Integrated_DistSamp.
455 The results presented in this paper were created using version 1.3 of the code (ChloerNater
456 et al. 2024).

457 Supplementary figures and posterior samples from the model run on the real data are
458 available as a time-stamped open archived on Open Science Framework (Nilsen and Nater
459 2024).

460

461 **References**

- 462 Andersen, O., B. P. Kaltenborn, J. Vitterso, and T. Willebrand. 2014. "Preferred Harvest
463 Principles and - Regulations Amongst Willow Ptarmigan Hunters in Norway." Journal
464 Article. *Wildlie Biology* 20 (5): 285–90. <https://doi.org/10.2981/wlb.00048>.
- 465 Beng, K. C., and R. T. Corlett. 2022. "Applications of Environmental DNA (eDNA) in Ecology
466 and Conservation: Opportunities, Challenges and Prospects." *Biodiversity and Conservation*
467 29: 2089–2121. <https://doi.org/10.1007/s10531-020-01980-0>.
- 468 Bowler, D. E., M. A. J. Kvasnes, H. C. Pedersen, B. K. Sandercock, and E. B. Nilsen. 2020.
469 "Impacts of Predator-Mediated Interactions Along a Climatic Gradient on the Population
470 Dynamics of an Alpine Bird." Journal Article. *Proc R Soc* 287 (1941): 20202653.
471 <https://doi.org/10.1098/rspb.2020.2653>.
- 472 Buckland, Stephen T, Eric A Rexstad, Tiago André Marques, Cornelia Sabrina Oedekoven, et
473 al. 2015. *Distance Sampling: Methods and Applications*. Vol. 431. Springer.
- 474 Caswell, Hal. 2000. *Matrix Population Models*. Vol. 1. Sinauer Sunderland, MA.
- 475 ChloeRNater, ErlendNilsen, christofferhohi, Matthew Grainger, and Bernardo Brandão
476 Niebuhr. 2024. "ErlendNilsen/OpenPop_Integrated_DistSamp: Ptarmigan IDSM v1.3."
477 Zenodo. <https://doi.org/10.5281/zenodo.10462269>.
- 478 Cornulier, Thomas, Nigel G. Yoccoz, Vincent Bretagnolle, Jon E. Brommer, Alain Butet,
479 Frauke Ecke, David A. Elston, et al. 2013. "Europe-Wide Dampening of Population Cycles in
480 Keystone Herbivores." Journal Article. *Science* 340 (6128): 63–66.
481 <https://doi.org/10.1126/science.1228992>.
- 482 Danielsen, Finn, Hajo Eicken, Mikkel Funder, Noor Johnson, Olivia Lee, Ida Theilade,
483 Dimitrios Argyriou, and Neil D. Burgess. 2022. "Community Monitoring of Natural Resource
484 Systems and the Environment." *Annual Review of Environment and Resources* 47 (1): 637–
485 70. <https://doi.org/10.1146/annurev-environ-012220-022325>.
- 486 Eriksen, Lasse Frost, Thor Harald Ringsby, Hans Chr. Pedersen, and Erlend B. Nilsen. 2023.
487 "Climatic Forcing and Individual Heterogeneity in a Resident Mountain Bird: Legacy Data
488 Reveal Effects on Reproductive Strategies." *Royal Society Open Science* 10 (5): 221427.
489 <https://doi.org/doi:10.1098/rsos.221427>.
- 490 Hagen, Yngvar. 1952. *Rovfuglene Og Viltpleien*. Gyldendal Norsk forlag.
- 491 Hamel, S., S. T. Killengreen, J. A. Henden, N. E. Eide, L. Roed-Eriksen, R. A. Ims, and N. G.
492 Yoccoz. 2013. "Towards Good Practice Guidance in Using Camera-Traps in Ecology:
493 Influence of Sampling Design on Validity of Ecological Inferences." Journal Article. *Methods*
494 *in Ecology and Evolution* 4 (2): 105–13. [https://doi.org/DOI 10.1111/j.2041-](https://doi.org/DOI 10.1111/j.2041-210x.2012.00262.x)
495 [210x.2012.00262.x](https://doi.org/DOI 10.1111/j.2041-210x.2012.00262.x).
- 496 Hjeljord, Olav, and Leif Egil Loe. 2022. "The Roles of Climate and Alternative Prey in
497 Explaining 142 Years of Declining Willow Ptarmigan Hunting Yield." Journal Article. *Wildlie*
498 *Biology* 2022 (6): e01058. <https://doi.org/https://doi.org/10.1002/wlb3.01058>.

- 499 Israelsen, Markus F, Lasse F Eriksen, Pål F Moa, Bjørn Roar Hagen, and Erlend B Nilsen.
500 2020. "Survival and Cause-Specific Mortality of Harvested Willow Ptarmigan (*Lagopus*
501 *Lagopus*) in Central Norway." *Ecology and Evolution* 10 (20): 11144–54.
502 <https://doi.org/10.1002/ece3.6754>.
- 503 Kausrud, K. L., A. Mysterud, H. Steen, J. O. Vik, E. Ostbye, B. Cazelles, E. Framstad, et al. 2008.
504 "Linking Climate Change to Lemming Cycles." Journal Article. *Nature* 456 (7218): 93–U3.
505 <https://doi.org/10.1038/nature07442>.
- 506 Kissling, W. Daniel, Jorge A. Ahumada, Anne Bowser, Miguel Fernandez, Néstor Fernández,
507 Enrique Alonso García, Robert P. Guralnick, et al. 2018. "Building Essential Biodiversity
508 Variables (EBVs) of Species Distribution and Abundance at a Global Scale." Journal Article
509 93 (1): 600–625. <https://doi.org/10.1111/brv.12359>.
- 510 Kvasnes, M. A. J., H. C. Pedersen, and E. B. Nilsen. 2018. "Quantifying Suitable Late Summer
511 Brood Habitats for Willow Ptarmigan in Norway." Journal Article. *BMC Ecology* 18 (1): 41.
512 <https://doi.org/10.1186/s12898-018-0196-6>.
- 513 Kvasnes, M. A. J., H. C. Pedersen, T. Storaas, and E. B. Nilsen. 2014. "Large-Scale Climate
514 Variability and Rodent Abundance Modulates Recruitment Rates in Willow Ptarmigan
515 (*Lagopus Lagopus*)." Journal Article. *Journal of Ornithology* 155 (4): 891–903.
516 <https://doi.org/10.1007/s10336-014-1072-6>.
- 517 Kvasnes, M. A. J., Hans Chr. Pedersen, H. Solvang, T. Storaas, and Erlend B. Nilsen. 2014.
518 "Spatial Distribution and Settlement Strategies in Willow Ptarmigan." Journal Article.
519 *Population Ecology* 57 (1): 151–61. <https://doi.org/10.1007/s10144-014-0454-1>.
- 520 Moore, Jeffrey E, and Jay Barlow. 2011. "Bayesian State-Space Model of Fin Whale
521 Abundance Trends from a 1991–2008 Time Series of Line-Transect Surveys in the
522 California Current." *Journal of Applied Ecology* 48 (5): 1195–205.
- 523 Nilsen, E. B., and C. R. Nater. 2024. "Supplementary Information to "an Integrated Open
524 Population Distance Sampling Approach for Modelling Age-Structured Populations."
525 Archive. <https://doi.org/10.17605/OSF.IO/TPRV2>.
- 526 Nilsen, E. B., and O. Strand. 2018. "Integrating Data from Multiple Sources for Insights into
527 Demographic Processes: Simulation Studies and Proof of Concept for Hierarchical Change-
528 in-Ratio Models." Journal Article. *PLoS One* 13 (3): e0194566.
529 <https://doi.org/10.1371/journal.pone.0194566>.
- 530 Nilsen, E. B., R. Vang, M. Kjøsberg, and M. A. J. Kvasnes. 2023. "Tetraonid Line Transect
531 Surveys from Norway: Data from Fjellstyrene." Dataset. <https://doi.org/10.15468/975ski>.
- 532 R Core Team. 2023. *R: A Language and Environment for Statistical Computing*. Vienna,
533 Austria: R Foundation for Statistical Computing. <https://www.R-project.org/>.
- 534 Sandercock, Brett, Erlend B Nilsen, Henrik Brøseth, and Hans Chr Pedersen. 2011. "Is
535 Hunting Mortality Additive or Compensatory to Natural Mortality? Effects of Experimental

- 536 Harvest on the Survival and Cause-Specific Mortality of Willow Ptarmigan.” *Journal of*
537 *Animal Ecology* 80 (1): 244–58. <https://doi.org/10.1111/j.1365-2656.2010.01769.x>.
- 538 Schaub, Michael, and Marc Kery. 2021. *Integrated Population Models: Theory and Ecological*
539 *Applications with r and JAGS*. Academic Press.
- 540 Schmidt, Joshua H, and Hillary L Robison. 2020. “Using Distance Sampling-Based Integrated
541 Population Models to Identify Key Demographic Parameters.” *The Journal of Wildlife*
542 *Management* 84 (2): 372–81.
- 543 Skalski, John, Kristin Ryding, and Joshua Millspaugh. 2005. *Wildlife Demography: Analysis of*
544 *Sex, Age, and Count Data*. Academic Press.
- 545 Sollmann, Rahel, Beth Gardner, Richard B Chandler, J Andrew Royle, and T Scott Sillett.
546 2015. “An Open-Population Hierarchical Distance Sampling Model.” *Ecology* 96 (2): 325–31.
- 547 Steen, J. B., H. Steen, N. C. Stenseth, S. Myrberget, and V. Marcström. 1988. “Microtine
548 Density and Weather as Predictors of Chick Production in Willow Ptarmigan, *Lagopus*
549 *Lagopus*.” Journal Article. *Oikos* 51 (3): 367–73. <Go to ISI>://A1988M692300016 .
- 550 Valpine, Perry de, Daniel Turek, Christopher J Paciorek, Clifford Anderson-Bergman,
551 Duncan Temple Lang, and Rastislav Bodik. 2017. “Programming with Models: Writing
552 Statistical Algorithms for General Model Structures with NIMBLE.” *Journal of Computational*
553 *and Graphical Statistics* 26 (2): 403–13.
- 554 Wieczorek, David AND Guralnick, John AND Bloom. 2012. “Darwin Core: An Evolving
555 Community-Developed Biodiversity Data Standard.” *PLOS ONE* 7 (January): 1–8.
556 <https://doi.org/10.1371/journal.pone.0029715>.
- 557 Williams, Byron K, James D Nichols, and Michael J Conroy. 2002. *Analysis and Management*
558 *of Animal Populations*. Academic press.
- 559 Zipkin, Elise F, Erin R Zylstra, Alexander D Wright, Sarah P Saunders, Andrew O Finley,
560 Michael C Dietze, Malcolm S Itter, and Morgan W Tingley. 2021. “Addressing Data
561 Integration Challenges to Link Ecological Processes Across Scales.” Journal Article 19 (1):
562 30–38. <https://doi.org/https://doi.org/10.1002/fee.2290>.